# Electronic correlation-driven orbital polarization transitions in the orbital-selective Mott compound $Ba_2CuO_{4-\delta}$

Yu Ni,[1] Ya-Min Quan,[2] Jingyi Liu,[1] Yun Song,[1,*] and Liang-Jian Zou[2,†]

[1]*Department of Physics, Beijing Normal University, Beijing 100875, China*

[2]*Key Laboratory of Materials Physics, Institute of Solid State Physics, Chinese Academy of Sciences, P. O. Box 1129, Hefei 230031, China*

(Received 20 December 2019; revised 8 February 2021; accepted 1 June 2021; published 14 June 2021)

The electronic states near the Fermi level of recently discovered superconductor $Ba_2CuO_{4-\delta}$ consist primarily of the Cu $d_{x^2-y^2}$ and $d_{3z^2-r^2}$ orbitals. We investigate the electronic correlation effect and the orbital polarization of an effective two-orbital Hubbard model mimicking the low-energy physics of $Ba_2CuO_{4-\delta}$ in the hole-rich regime by utilizing the dynamical mean-field theory with the Lanczos method as the impurity solver. We find that the hole-overdoped $Ba_2CuO_{4-\delta}$ with $3d^8$ ($Cu^{3+}$) is in the orbital-selective Mott phase (OSMP) at half-filling, and the typical two-orbital feature remains in $Ba_2CuO_{4-\delta}$ when the electron filling approaches $n_e \sim 2.5$, which closely approximates to the experimental hole doping for the emergence of the high-$T_c$ superconductivity. We also obtain that the orbital polarization is very stable in the OSMP, and the multiorbital correlation can drive orbital polarization transitions. These results indicate that in hole-overdoped $Ba_2CuO_{4-\delta}$ the OSMP physics and orbital polarization, local magnetic moment, and spin or orbital fluctuations still exist. We propose that our present results are also applicable to $Sr_2CuO_{4-\delta}$ and other two-orbital cuprates, demanding an unconventional multiorbital superconducting scenario in hole-overdoped high-$T_c$ cuprates.

DOI: 10.1103/PhysRevB.103.214510

## I. INTRODUCTION

The involvement of two Cu $3d$ orbitals in the superconducting (SC) states in the recently discovered high-$T_c$ superconducting (HTSC) compound $Ba_2CuO_{4-\delta}$ with $T_c = 73$ K [1], as well as the early discovered compound $Sr_2CuO_{4-\delta}$ with $T_c = 95$ K [2–4], greatly challenges the prevailing single-orbital scenario in conventional HTSC cuprates. In the previous cuprates $La_2CuO_4$, and $YBa_2Cu_3O_6$, etc., the parent phases of these undoped compounds are charge transfer insulator or Mott insulator, where the active Cu $3d_{x^2-y^2}$ orbital is singly occupied and the ground state is Néel antiferromagnetic insulator. Once holes are doped into the O $2p_x$ and $2p_y$ orbitals, the strong O $2p$-Cu $3d$ hybridization and large charge transfer gap form the Zhang-Rice singlet [5], and an effective single-orbital $t$-$J$ model is proposed for describing the low-energy physics of doped cuprates [6]. Such an effective single-orbital scenario addressed many experimental results [7], demonstrating the reasonability of the model. The essential electronic states in $Ba_2CuO_{4-\delta}$ do not fall into this scenario: first, neither $Ba_2CuO_3$ nor $Ba_2CuO_4$ is a charge transfer insulator, instead, its charge transfer gap is rather small; second, both the Cu $3d_{3z^2-r^2}$ and $3d_{x^2-y^2}$ orbitals appear near the Fermi energy in SC $Ba_2CuO_{4-\delta}$ [1]. This suggests that $Ba_2CuO_{4-\delta}$ is a multiorbital superconductor. This scenario, which is completely different from that of the well-known $t$-$J$ model, brings about the assumptions of two SC dome phases and orbital selective superconductivity [8,9].

The detail inspections to the electronic properties of $Ba_2CuO_{4-\delta}$ will provide new insight or even new scenario, especially the electronic states of SC $Ba_2CuO_{4-\delta}$ lie in $Ba_2CuO_4$ and in $Ba_2CuO_3$. It is well known that $La_2CuO_4$ and derivative cuprates are strongly correlated systems. We expect that $Ba_2CuO_{4-\delta}$ is a correlated system, though it can be viewed as a hole-overdoped compound. Recently, Liu *et al.* proposed that $Ba_2CuO_3$ is an antiferromagnetic insulator [10] and should be the parent phase; however, Maier *et al.* suggested that $Ba_2CuO_4$ should be the parent phase [8]. To resolve such a dispute, it is crucial to clarify the role of the electronic correlation in $Ba_2CuO_{4-\delta}$ in the hole-rich regime. Correspondingly, one may also ask what the role of Hund's rule coupling plays in such a multiorbital system and how the quantum phases evolve with increasing hole concentration [8–12]. These issues are important since orbital and magnetic fluctuations are closely related to the ground-state magnetism.

On the other hand, we notice that compared with antiferromagnetically insulating $Ba_2CuO_3$, $Ba_2CuO_4$ exhibits a paramagnetically metallic ground state [10], though it is stoichiometric $3d^7$ configuration. How can such a paramagnetically metallic phase be stable in an integer-filling correlated electron system? At present it is not clear that what role the electronic correlation plays in the paramagnetically metallic ground states of $Ba_2CuO_4$. Meanwhile, the orbital polarization character of the hole-overdoped $Ba_2CuO_{4-\delta}$, which is essential for SC pairing symmetry, is also profoundly affected by the electronic correlation. These facts urge us to clarify the role of electronic correlations in the two-orbital compound $Ba_2CuO_{4-\delta}$, as well as $Sr_2CuO_{4-\delta}$.

In this paper we use the dynamical mean-field theory (DMFT) [13–15] with the Lanczos method as its impurity

*yunsong@bnu.edu.cn
†zou@theory.issp.ac.cn

 

solver to investigate the influences of Coulomb correlation and hole doping on the electronic states in a two-orbital Hubbard model, which is applicable for the compressed $Ba_2CuO_{4-\delta}$ compound. Our results suggest that $Ba_2CuO_{4-\delta}$ compound has a typical two-orbital character, even when the electron filling approaches $n_e \sim 2.5$, which is very close to the optimal hole doping of the high-$T_c$ superconducting phase [1]. We demonstrate that the hole-overdoped $Ba_2CuO_{4-\delta}$ is in the orbital-selective Mott phase (OSMP) at half-filling with two electrons in the two $e_g$ orbitals, which is regarded as the parent phase of $Ba_2CuO_{4-\delta}$ compound. Our results also show that the orbital polarization is extremely stable in the OSMP region, providing a direct evidence for the occurrence of the OSMP. The orbital polarization transitions can be driven by the multiorbital correlations in the $Ba_2CuO_{4-\delta}$, especially in the hole-rich region.

This paper is organized as follows. In Sec. II we introduce a two-orbital Hubbard model for the hole-overdoped $Ba_2CuO_{4-\delta}$, and we explain the numerical method adopted in our study: the DMFT approach with the Lanczos solver. In Sec. III we demonstrate the effects of electronic correlation and hole doping on the electronic states by analyzing the phase diagrams of the hole-overdoped $Ba_2CuO_{4-\delta}$. The principal findings of this paper are summarized in Sec. IV.

## II. MODEL AND METHOD

On account of the crossing to the Fermi energy for both the two bands formed from the Cu $3d_{x^2-y^2}$ and $3d_{3z^2-r^2}$ orbitals of the compressed $Ba_2CuO_{4-\delta}$ compound, we investigate the electronic states described by a two-orbital Hamiltonian $H = H_t + H_I$, where the tight-binding (TB) Hamiltonian $H_t$ reads [8]

$$H_t = -\sum_{ij}\sum_{l\sigma} t_{ll}^{(ij)} d_{il\sigma}^{\dagger} d_{jl\sigma} - \sum_{ij}\sum_{l\neq l',\sigma} t_{ll'}^{(ij)} d_{il\sigma}^{\dagger} d_{jl'\sigma} + \sum_{il\sigma}(\epsilon_l - \mu) d_{il\sigma}^{\dagger} d_{il\sigma}. \quad (1)$$

$d_{il\sigma}^{\dagger}$ ($d_{il\sigma}$) is an electron creation (annihilation) operator for orbital $l$ (=1 for $d_{x^2-y^2}$ and 2 for $d_{3z^2-r^2}$) at site $i$ with spin $\sigma$. $t_{11/22}^{(ij)}$ and $t_{12}^{(ij)}$ represent the intraorbital and interorbital hoppings between sites $i$ and $j$, respectively. $\epsilon_l$ represents the on-site energy of orbital $l$, and the crystal-field splitting is given as $\epsilon_d = \epsilon_1 - \epsilon_2$. $\mu$ denotes the chemical potential.

The interaction Hamiltonian $H_I$ is exactly the same as the correlation part of the standard two-orbital Hubbard model [16,17],

$$H_I = \frac{U}{2}\sum_{il\sigma} n_{il\sigma} n_{il\bar{\sigma}} + \sum_{i,l<l',\sigma\sigma'} (U' - \delta_{\sigma\sigma'} J_H) n_{il\sigma} n_{il'\sigma'} + \frac{J_H}{2}\sum_{i,l\neq l',\sigma} d_{il\sigma}^{\dagger} d_{il\bar{\sigma}}^{\dagger} d_{il'\bar{\sigma}} d_{il'\sigma} + \frac{J_H}{2}\sum_{i,l\neq l',\sigma\sigma'} d_{il\sigma}^{\dagger} d_{il'\sigma'}^{\dagger} d_{il\sigma'} d_{il'\sigma}, \quad (2)$$

where $U$ ($U'$) corresponds to the intraorbital (interorbital) interaction, and $J_H$ is the Hund's rule coupling. For the systems with spin rotation symmetry, we have $U = U' + 2J_H$.

TABLE I. Model parameters of the TB Hamiltonian of $Ba_2CuO_{4-\delta}$ at half-filling in eV [8].

| | on-site energy ($\epsilon$) | 1st hopping ($t$) | 2nd hopping ($t'$) | 3rd hopping ($t''$) |
|---|---|---|---|---|
| orbital $d_{x^2-y^2}$ | −0.222 | 0.504 | −0.067 | 0.130 |
| orbital $d_{3z^2-r^2}$ | 0.661 | 0.196 | 0.026 | 0.029 |
| interorbital | 0 | −0.302 | 0 | −0.051 |

$Ba_2CuO_{4-\delta}$ can be viewed as a hole-overdoped compound. The nominal 2(1-$\delta$) holes per Cu are doped in the $Ba_2CuO_{4-\delta}$ compound [1], giving a relation between $\delta$ and the hole concentration $x_h$ as $\delta = 1 - x_h/2$. Accordingly, the copper valence can be expressed as $Cu^{2+x_h}$ for a hole concentration $x_h$ [8]. At half-filling with $\delta = 0.5$, there are two electrons in the $d_{x^2-y^2}$ and $d_{3z^2-r^2}$ orbitals of $Cu^{3+}$ in $Ba_2CuO_{4-\delta}$.

Based on the DFT-calculated band structures of the compressed $Ba_2CuO_{4-\delta}$ compound with hole concentration $x_h = 1$ [8], the model parameters of the TB Hamiltonian $H_t$ in Eq. (1) are given in Table I, including the hopping parameters for the first ($t$), second ($t'$), and third ($t''$) nearest neighbors, as well as the on-site energy $\epsilon_l$. Through the Fourier transformation, $H_t$ is changed to

$$H_0(k) = \sum_{k\sigma}\sum_{ll'} \{\xi_{ll'}(k) + [\epsilon_l - \mu]\delta_{ll'}\} d_{l\sigma}^{\dagger}(k) d_{l'\sigma}(k), \quad (3)$$

with

$$\xi_{11/22}(k) = 2t_{11/22}(\cos k_x + \cos k_y) + 4t'_{11/22}\cos k_x \cos k_y + 2t''_{11/22}(\cos 2k_x + \cos 2k_y), \quad (4)$$

and

$$\xi_{12}(k) = \xi_{21}(k) = 2t_{12}(\cos k_x - \cos k_y) + 2t''_{12}(\cos 2k_x - \cos 2k_y). \quad (5)$$

The energy of the $d_{3z^2-r^2}$ orbital varies as $\epsilon_2 = 0.661 - 5(1 - x_h)$ with decreasing hole concentration $x_h$, while the energy $\epsilon_1$ of the orbital $d_{x^2-y^2}$ is kept as a constant [8]. For the conditions with $x_h < 1$, the chemical potential $\mu$ has been adjusted to keep an electron filling $n_e = 1 + 2\delta$ ($n_e = 3 - x_h$) for the hole-overdoped $Ba_2CuO_{4-\delta}$.

We map the lattice Hamiltonian on to an impurity model with fewer degrees of freedom,

$$H_{\rm imp} = \sum_{ml\sigma} \varepsilon_{ml\sigma} c_{ml\sigma}^{\dagger} c_{ml\sigma} + \sum_{l\sigma}(\epsilon_l - \mu) d_{l\sigma}^{\dagger} d_{l\sigma} + \sum_{ll'm\sigma} V_{ll'm\sigma}(d_{l\sigma}^{\dagger} c_{ml'\sigma} + c_{ml'\sigma}^{\dagger} d_{l\sigma}) + H_I^{\rm imp} \quad (6)$$

with

$$H_I^{\rm imp} = \frac{U}{2}\sum_{l\sigma} n_{l\sigma} n_{l\bar{\sigma}} + \sum_{l<l',\sigma\sigma'} (U' - \delta_{\sigma\sigma'} J_H) n_{l\sigma} n_{l'\sigma'} + \frac{J_H}{2}\sum_{l\neq l',\sigma} d_{l\sigma}^{\dagger} d_{l\bar{\sigma}}^{\dagger} d_{l'\bar{\sigma}} d_{l'\sigma} + \frac{J_H}{2}\sum_{l\neq l',\sigma\sigma'} d_{l\sigma}^{\dagger} d_{l'\sigma'}^{\dagger} d_{l\sigma'} d_{l'\sigma}, \quad (7)$$

where $c^{\dagger}_{ml\sigma}$ ($c_{ml\sigma}$) denotes the creation (annihilation) operator for the bath lattice of orbital $l$, $\varepsilon_{ml\sigma}$ denotes the energy of the $m$th environmental bath of orbital $l$, and $V_{ll'm\sigma}$ represents the coupling between the orbital $l$ of the impurity site and environmental bath of orbital $l'$.

The Green's function of the two-orbital impurity model can be expressed as a $2 \times 2$ matrix,

$$\boldsymbol{G}_{\rm imp}(i\omega_n) = \begin{pmatrix} G_{11}(i\omega_n) & G_{12}(i\omega_n) \\ G_{21}(i\omega_n) & G_{22}(i\omega_n) \end{pmatrix}. \tag{8}$$

The Green's function $\boldsymbol{G}_{\rm imp}$ at zero temperature is calculated by the Lanczos solver [18–20]. We choose a bath size $n_b = 3$ in our calculations. It has been proved that the critical values of the OSMT in a two-orbital Hubbard model are almost the same when the bath size is taken as $n_b \geqslant 3$ in the DMFT calculations with Lanczos solver [21].

In the Lanczos procedure [18], the diagonal matrix elements of the Green's function $G_{ll}$ are expressed as

$$G_{ll}(\omega) = G^{(+)}_{ll}(\omega) + G^{(-)}_{ll}(\omega), \tag{9}$$

where

$$G^{(+)}_{ll}(\omega) = \cfrac{\langle\phi_0|d_l d_l^{\dagger}|\phi_0\rangle}{\omega - a_0^{(+)} - \cfrac{b_1^{(+)2}}{\omega - a_1^{(+)} - \cfrac{b_2^{(+)2}}{\omega - a_2^{(+)} - \ldots}}}, \tag{10}$$

and

$$G^{(-)}_{ll}(\omega) = \cfrac{\langle\phi_0|d_l^{\dagger} d_l|\phi_0\rangle}{\omega + a_0^{(-)} - \cfrac{b_1^{(-)2}}{\omega + a_1^{(-)} - \cfrac{b_2^{(-)2}}{\omega + a_2^{(-)} - \ldots}}}. \tag{11}$$

$|\phi_0\rangle$ is the ground state. $a_n^{(+)}$ and $b_n^{(+)}$ are the elements of tridiagonal form of the Hamiltonian matrix, constructed from the initial state $d_l^{\dagger}|\phi_0\rangle/\sqrt{\langle\phi_0|d_l d_l^{\dagger}|\phi_0\rangle}$, and $a_n^{(-)}$ and $b_n^{(-)}$ are correspondingly obtained by another initial state $d_l|\phi_0\rangle/\sqrt{\langle\phi_0|d_l^{\dagger} d_l|\phi_0\rangle}$. The off-diagonal elements $G_{12}$ and $G_{21}$ can be also obtained by the Lanczos method, based on the relation

$$\begin{aligned} G_{12}(i\omega_n) &= G_{21}(i\omega_n) \\ &= \frac{1}{2}\left[G_{1+2,1+2}(i\omega_n) - \sum_l G_{ll}(i\omega_n)\right], \end{aligned} \tag{12}$$

where $G_{1+2,1+2}$ is a combined Green's function, $G_{1+2,1+2} = \langle\langle d_1 + d_2 | d_1^{\dagger} + d_2^{\dagger}\rangle\rangle$, which is calculated in the Lanczos method by replacing the operators $d_l^{\dagger}$ and $d_l$ as $d_1^{\dagger} + d_2^{\dagger}$ and $d_1 + d_2$, respectively.

The Weiss function of the impurity model can be obtained through the parameters of the impurity Hamiltonian by

$$\boldsymbol{\mathcal{G}}_0^{\rm imp}(i\omega_n)^{-1} = (i\omega_n + \mu)\boldsymbol{I} - \boldsymbol{\Delta}(i\omega_n), \tag{13}$$

where $\boldsymbol{\mathcal{G}}_0^{\rm imp}(i\omega_n)$ and $\boldsymbol{\Delta}(i\omega_n)$ are $2 \times 2$ matrices, and symbol $\boldsymbol{I}$ denotes the identity matrix. The hybridization matrix $\boldsymbol{\Delta}(i\omega_n)$ is defined as

$$\boldsymbol{\Delta}(i\omega_n) = \begin{pmatrix} \Delta_{11}(i\omega_n) & \Delta_{12}(i\omega_n) \\ \Delta_{21}(i\omega_n) & \Delta_{22}(i\omega_n) \end{pmatrix}, \tag{14}$$

with

$$\Delta_{l_1 l_2}(i\omega_n) \equiv \sum_{ml} \frac{V_{l_1 lm} V_{l_2 lm}}{i\omega_n - \varepsilon_{ml}}. \tag{15}$$

We calculate the $2 \times 2$ self-energy matrix $\boldsymbol{\Sigma}_{\rm imp}(i\omega_n)$ of the impurity Hamiltonian by the Dyson equation

$$\boldsymbol{\Sigma}_{\rm imp}(i\omega_n) = \boldsymbol{\mathcal{G}}_0^{\rm imp}(i\omega_n)^{-1} - \boldsymbol{G}_{\rm imp}(i\omega_n)^{-1}, \tag{16}$$

and the $2 \times 2$ lattice Green's function matrix $\boldsymbol{G}_{lat}(i\omega_n)$ is obtained by

$$\begin{aligned} \boldsymbol{G}_{lat}(i\omega_n) &= \frac{1}{N}\sum_k \boldsymbol{G}(i\omega_n, k) \\ &= \frac{1}{N}\sum_k \frac{1}{i\omega_n \boldsymbol{I} - \boldsymbol{H}_0(k) - \boldsymbol{\Sigma}_{\rm imp}(i\omega_n)}, \end{aligned} \tag{17}$$

where $\boldsymbol{H}_0$ is the matrix representation of Eq. (3).

We build the DMFT self-consistent loop with $\boldsymbol{G}_{\rm imp}(i\omega_n) = \boldsymbol{G}_{lat}(i\omega_n)$ to determine the parameters $\varepsilon_{ml}$ and $V_{ll'm}$. Analytic continuation is also performed to obtain the real frequency Green's function $\boldsymbol{G}(\omega)$ [13].

We calculate the orbital-resolved spectral density of each orbital by

$$A_l(\omega) = -\frac{1}{\pi}{\rm Im}G^{(lat)}_{ll}(\omega + i\eta), \tag{18}$$

where $\eta$ is an energy broadening factor. Then, the orbital projected optical conductivity can be expressed approximately as

$$\begin{aligned} \sigma_l(\omega) = \pi \int_{-\infty}^{\infty} d\epsilon D_l(\epsilon) \int_{-\infty}^{\infty} \frac{d\omega'}{2\pi} A_l(\omega') A_l(\omega' + \omega) \\ \times \frac{n_f^{(l)}(\omega') - n_f^{(l)}(\omega' + \omega)}{\omega}, \end{aligned} \tag{19}$$

where $n_f(\omega)$ is the Fermi function, and $D_l$ represents the density of states (DOS) of the TB Hamiltonian. We neglect the vertex correction to the current operator, and the off-diagonal elements are also neglected in our calculations.

To explore possible orbital polarization and orbital ordering in $Ba_2CuO_{4-\delta}$, we also calculate the local orbital squared moment $\langle T_z^2\rangle$ of the two orbitals by [22]

$$\left\langle T_z^2 \right\rangle = \left\langle \left(\hat{n}_{l_1} - \hat{n}_{l_2}\right)^2 \right\rangle, \tag{20}$$

from which we could obtain the evolution of orbital polarization with increasing electronic correlation.

## III. RESULTS AND DISCUSSIONS

We study the electronic states in $Ba_2CuO_{4-\delta}$ as the hole doping varies from intermediate doping region to highly overdoped region, and we also pay close attention to the optimal hole-doping region around the electron filling $n_e \sim 2.5$, where the high-$T_c$ superconductivity occurs in $Ba_2CuO_{4-\delta}$. First, we study the orbital selective Mott transition (OSMT) in the strongly overdoped system for $3d^8$ ($Cu^{3+}$) with two electrons in the two $e_g$ orbitals, i.e., at half-filling with $n_e = 2$, which is regarded as the parent phase of $Ba_2CuO_{4-\delta}$ compound.

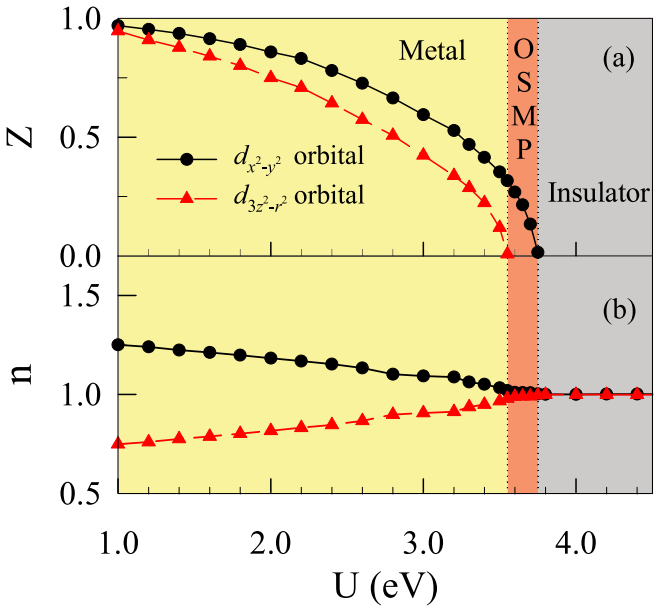


FIG. 1. (a) Orbital-resolved quasiparticle weight $Z_l$ and (b) electron occupation $n_l$ as a function of interaction $U$ when $J_H = 0.25U$ for $Ba_2CuO_{4-\delta}$ at half-filling. Between the metallic (yellow) and insulating (gray) phases, an OSMP (orange) occurs in a narrow interaction region with 3.55 eV $\leqslant U <$ 3.75 eV.

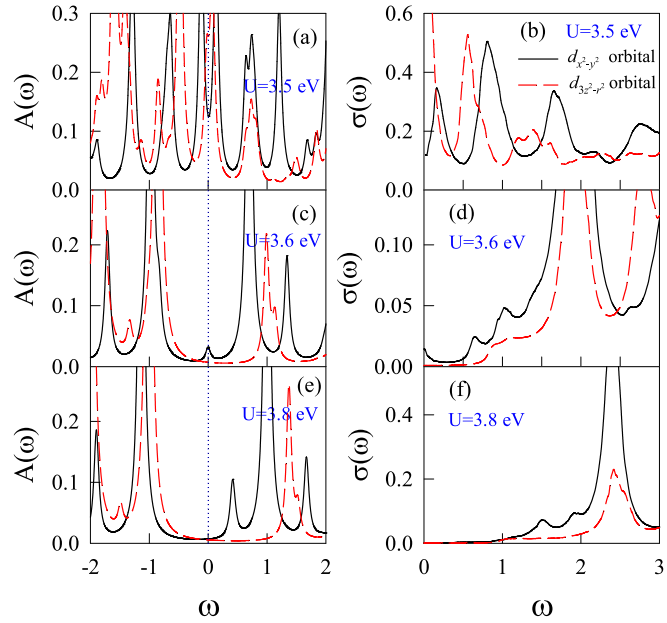


FIG. 2. Effect of interaction $U$ on the orbital-resolved spectral density $A_l(\omega)$ (left panel) and the corresponding orbital-dependent optical conductivity $\sigma_l(\omega)$ (right panel) of the two bands of $Ba_2CuO_{4-\delta}$ with $J_H = 0.25U$ at half-filling. The Fermi energy is denoted by a blue dotted line, and the energy broadening is given as $\eta = 0.05$ eV.

### A. OSMT at half-filling

Half-filled $Ba_2CuO_{4-\delta}$ with $n_e = 2$ displays prominent OSMP character under the correlated effect. In Fig. 1(a) we present the orbital-dependent quasiparticle weight $Z_l$, $Z_l = (1 - \frac{\partial}{\partial\omega}\mathrm{Re}\Sigma_l(\omega)|_{\omega=0})^{-1}$ [23], as a function of the intraorbital interaction $U$ when $J_H = 0.25U$ at half-filling. When $U <$ 3.55 eV, the two-band system is metallic with finite quasiparticle weights of the two orbitals. By contrast, the insulating phase with zero $Z_l$ is stable for both orbitals when $U >$ 3.75 eV. An OSMP occurs between the metallic and insulating phases with 3.55 eV $\leqslant U <$ 3.75 eV, in which the narrow $d_{3z^2-r^2}$ band behaves insulating, while the wide $d_{x^2-y^2}$ band is still metallic. The $U$ dependence of the electron occupations $n_l$ are shown in Fig. 1(b). We find that the electrons transfer from the wide $d_{x^2-y^2}$ band to the narrow $d_{3z^2-r^2}$ band with increasing $U$ at half-filling. Both bands become singly occupied ($n_l = 1$) after the OSMT, indicating that the two electrons in the two Cu $e_g$ orbitals distribute uniformly in both the OSMP and insulating phase, as observed in other degenerate two-orbital systems [24–27].

Figure 2 shows the orbital-resolved spectrum $A_l(\omega)$ and optical conductivity $\sigma_l(\omega)$ obtained in different phases. In the metallic phase with $U = 3.5$ eV, both bands have a finite spectral weight at the Fermi level, and there is a Drude peak in the optical conductivity accordingly, as shown in Figs. 2(a) and 2(b), respectively. At $U = 3.6$ eV a small resonance peak can be found in the DOS of the metallic wide $d_{x^2-y^2}$ band, accompanied with a small Drude peak in its optical conductivity. Meanwhile, a Mott gap opens around the Fermi level in the narrow $d_{3z^2-r^2}$ band, and the Drude weight is zero for its optical conductivity, demonstrating the well-defined OSMP character [28–30]. Insulating phase appears at $U = 3.8$ eV, where a Mott gap opens in the DOS and there is no Drude peak in the optical conductivity for both bands as shown in Figs. 2(e) and 2(f), respectively.

Decreasing the Hund's rule coupling to $J_H = 0.125U$, the Mott transitions in the two bands occur simultaneously at $U = U_{c1} = U_{c2} = 4.6$ eV, as shown in Fig. 3(a). This finding is in agreement with the early result that a large $J_H$

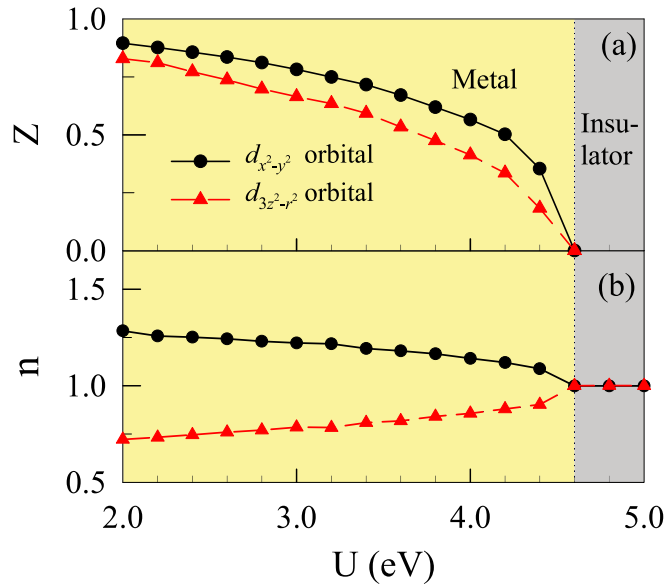


FIG. 3. (a) Quasiparticle weight and (b) electron occupation as a function of interaction $U$ when $J_H = 0.125U$ at half-filling. A direct transition from metallic phase to insulating phase is found.

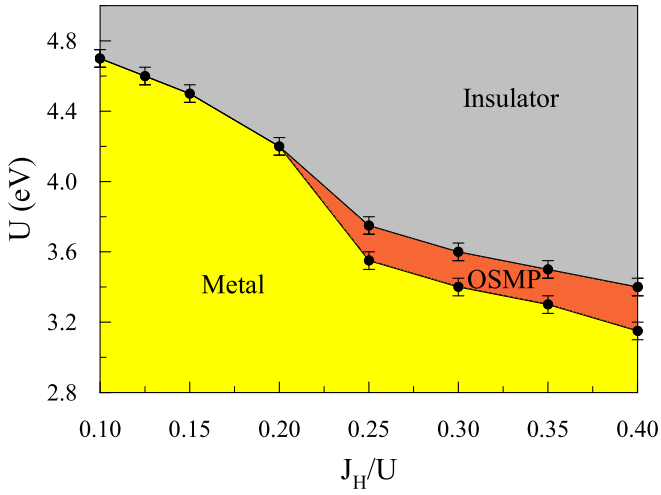


FIG. 4. Phase diagram of $Ba_2CuO_{4-\delta}$ at half-filling. The critical values of Mott transitions in the narrow and wide bands decrease with increasing $J_H/U$, leading the OSMP region to be wider accordingly. The OSMT vanishes if $J_H/U$ is smaller than 0.2.

promotes the OSMT at half-filling by strongly suppressing the coherence scale to block the orbital fluctuations [28,31–33]. Figure 3(b) shows that both bands become half-filled after the Mott transition.

We construct the $U$-$J_H$ phase diagram in Fig. 4. One observes that there exists a narrow region of the OSMP between the weakly correlated metallic phase and strongly correlated Mott insulating phase when $J_H > 0.2U$, which is getting to broaden with increasing $J_H$. It is obvious that large $J_H$ is beneficial to the occurrence of OSMP. The OSMP vanishes when $J_H < 0.2U$ because Coulomb correlation and Hund's rule coupling are inferior to the crystal-field splitting, in agreement with the previous results [31–34]. In the region of $J_H > 0.2U$, the system undergoes the transitions of a metallic phase to an OSMP and of an OSMP to an insulating phase as $U$ increases. Because $Ba_2CuO_{4-\delta}$ at half-filling is at least an intermediate correlated system [8], it should be an OSMP compound, or near the edge of the OSMP.

There have been two possibilities regarding the parent compound of the SC $Ba_2CuO_{4-\delta}$. One candidate is $Ba_2CuO_4$ [8], and the other one is $Ba_2CuO_3$ [10]. Our study suggests an alternative possibility that the half-filled $Ba_2CuO_{3.5}$ is the parent compound. Increasing the electron filling by removing some oxygens from $Ba_2CuO_{3.5}$, high-$T_c$ superconductivity emerges in $Ba_2CuO_{4-\delta}$ when $n_e \sim 2.5$ [1].

### B. Hole-overdoping effect

Focussing on the optimal hole doping for the occurrence of the high-$T_c$ superconductivity, in Fig. 5 we present the evolution of the orbital-resolved quasiparticle weight $Z_l$ with increasing multiorbital interactions $U$ and $J_H$ in $Ba_2CuO_{4-\delta}$ when the electron filling $n_e$ is around 2.5. Although the two bands are both good metal with large $Z_l$ in the weakly correlated region, a significant difference between the quasiparticle weight distributions for the two bands can be found in the strongly correlated region. It is obvious that the decline of the quasiparticle weight of the narrow $d_{3z^2-r^2}$ band is mainly

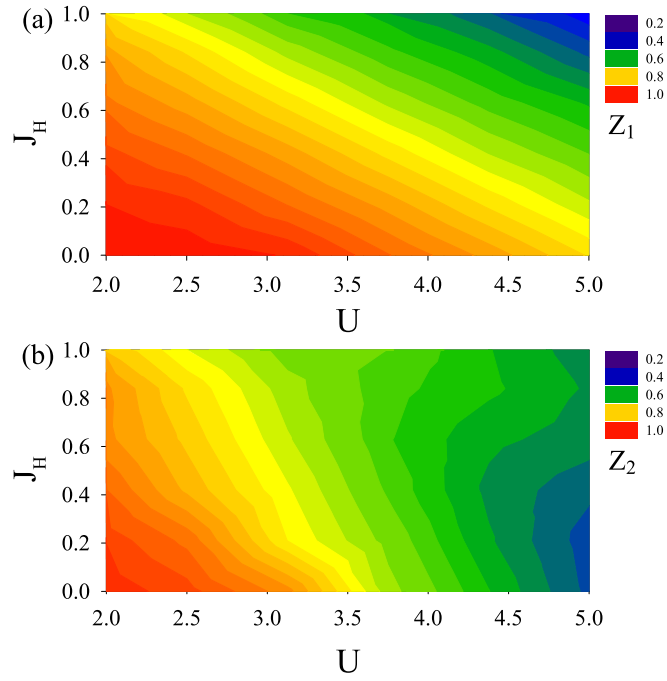


FIG. 5. Effects of Hund's rule coupling $J_H$ and interaction $U$ on quasiparticle weight $Z_l$ of the wide band $d_{x^2-y^2}$ (top panel) and the narrow band $d_{3z^2-r^2}$ (bottom panel) for $Ba_2CuO_{4-\delta}$ when $n_e \sim 2.5$.

driven by the intraorbital interaction $U$. On the other hand, a bad metallic character appears in the wide $d_{x^2-y^2}$ band when the Hund's rule coupling is strong enough. The two orbitals of $Ba_2CuO_{4-\delta}$ display different correlation features in the strongly correlated region when $n_e \sim 2.5$.

We present the spectral density $A_l(\omega)$ and electron occupation $n_l$ at different $J_H/U$ in Fig. 6. In Fig. 6(a) both bands have finite spectral weight at Fermi level and the system displays prominent metal character when $U = 2.4$ eV and $J_H = 0.5$ eV. With increasing correlations, we find two soft

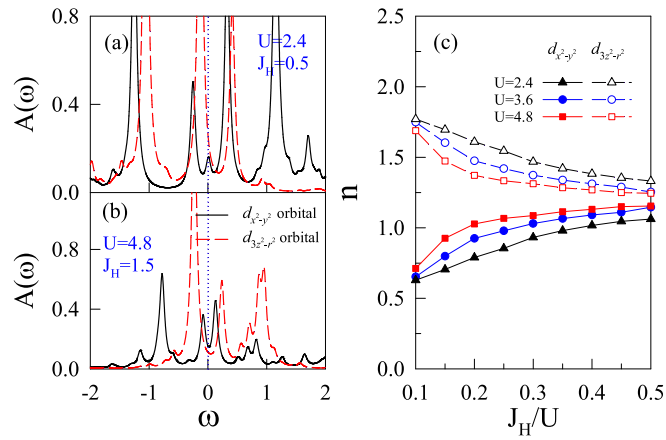


FIG. 6. Orbital-resolved spectral density $A_l(\omega)$ of $Ba_2CuO_{4-\delta}$ with $n_e \sim 2.5$ for different interactions: (a) $U = 2.4$ eV and $J_H = 0.5$ eV and (b) $U = 4.8$ eV and $J_H = 1.5$ eV. The energy broadening is $\eta = 0.05$ eV. (c) Orbital-resolved electron occupation $n_l$ as a function of $J_H/U$ for different interactions: $U = 2.4$ eV, 3.6 eV, and 4.8 eV when the electron filling $n_e$ is around 2.5.

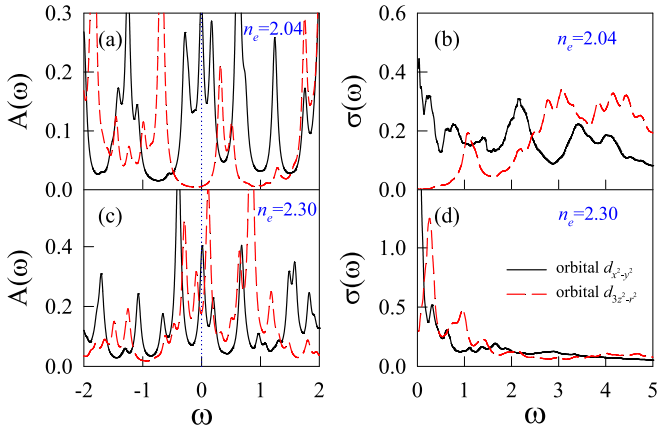


FIG. 7. The orbital-resolved spectral density $A_l(\omega)$ (left panel) and the corresponding orbital-dependent optical conductivity $\sigma_l(\omega)$ (right panel) on different electron filling $n_e$ of $Ba_2CuO_{4-\delta}$ when $J_H = 0.25U$ and $U = 3.6$ eV. The energy broadening is $\eta = 0.05$ eV.

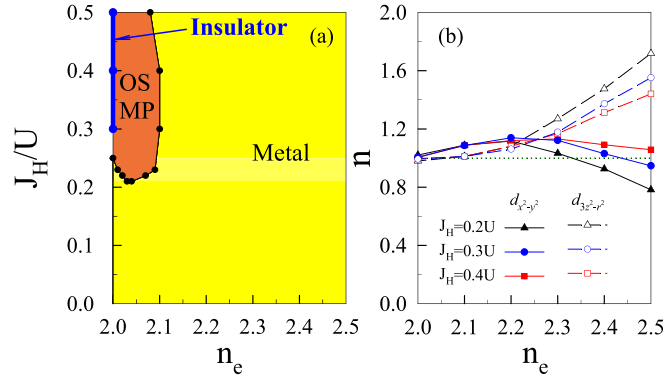


FIG. 8. (a) Phase diagram of $Ba_2CuO_{4-\delta}$ from the intermediate hole-doping region to the overdoped region with $2.0 \leqslant n_e < 2.5$ when $U = 3.6$ eV. (b) Orbital-resolved electron occupation as a function of $n_e$ for different $J_H$. The green dotted line indicates the half-filling of an orbital with $n = 1$. The OSMP occurs in a hole-rich regime $2.0 \leqslant n_e \leqslant 2.1$ for a not weak $J_H$, but the Mott insulating phase can only occur at half-filling with $n_e = 2.0$ when the Hund's rule coupling is larger as $J_H > 0.3U$.

gaps in the DOS of both orbitals when $U = 4.8$ eV and $J_H = 1.5$ eV shown in Fig. 6(b), indicating that the system becomes a bad metal in the strongly correlated region. We show the orbital-dependent electron occupation in Fig. 6(c) when the electron filling is around 2.5. Different from the results of half-filled systems shown in Figs. 1(b) and 3(b), electrons prefer to occupy the narrow $d_{3z^2-r^2}$ band. It is worth noticing that both $J_H$ and $U$ tend to uniformly distribute electrons within the two orbitals, and a finite Hund's rule coupling can make the wide $d_{x^2-y^2}$ band to be around half-filled, indicating that both orbitals have significant contributions. Therefore, our results give strong evidences of the two-orbital character in $Ba_2CuO_{4-\delta}$ when $n_e \sim 2.5$, which corresponds to the experimental hole-doping concentration for the occurrence of the high-$T_c$ superconductivity.

To find out the influence of the hole doping in $Ba_2CuO_{4-\delta}$, we extend our study to a wide doping region with $2.0 \leqslant n_e \leqslant 2.5$. In Fig. 7 we present the spectral density $A_l(\omega)$ and optical conductivity $\sigma_l(\omega)$ for different electron filling $n_e$ when $J_H = 0.25U$ and $U = 3.6$ eV, where the system should be in an OSMP at half-filling ($n_e = 2$) based on the phase diagram shown in Fig. 4. When we change the electron filling to $n_e = 2.04$, a Mott gap still opens in the narrow $d_{3z^2-r^2}$ band and its optical conductivity is zero at $\omega = 0$ correspondingly, as shown in Figs. 7(a) and 7(b). Also, the wide $d_{x^2-y^2}$ band has a finite resonance peak and a large Drude peak, indicating that the wide band is in a metallic phase. This indicates that an OSMP also occurs near half-filling. When the electron filling is changed to $n_e = 2.3$, the finite spectral weights at Fermi level and the large Drude peaks for both bands indicate that $Ba_2CuO_{4-\delta}$ transfers to a metallic phase, as shown in Figs. 7(c) and 7(d).

In the phase diagram shown in Fig. 8(a), an OSMP is found in a highly overdoped region near half-filling, which looks like an OSMP peninsula in the sea of metallic phase. If the electron filling $n_e$ is more than 2.1, $Ba_2CuO_{4-\delta}$ with $U = 3.6$ eV can only be a metal no matter how large the Hund's rule coupling is. On the other hand, the Mott insulating phase occurs only at half-filling with a strong Hund's rule coupling as $J > 0.3U$. The critical value $J_H^c$ for the OSMT takes the minimum value at $n_e \approx 2.04$. Besides, the disappearance of the OSMP when $J_H \leqslant 0.2U$ provides further evidence that the Hund's rule coupling can promote the OSMT [35], even away from half-filling. Although the difference between the electron occupancies of the two orbitals increases with increasing $n_e$, as shown in Fig. 8(b), the wide $d_{x^2-y^2}$ band is still approximately half-filled with $n_1 \approx 0.95$ when $n_e = 2.5$ and $J_H = 0.3U$. Our calculations demonstrate that $Ba_2CuO_{4-\delta}$ compound displays a typical two-orbital character from the intermediate hole-doping region to the overdoped region, including the optimal doping $n_e \sim 2.5$ for the occurrence of the high-$T_c$ superconductivity. In Sec. III C, we detect the correlation driven orbital polarization transitions in $Ba_2CuO_{4-\delta}$, resulting from the electron transfer between the two orbitals.

### C. Orbital polarization

In Fig. 9 we present the local orbital squared moment $\langle T_z^2 \rangle$ as a function of the intraorbital interaction $U$ at half-filling. The model Hamiltonian employed in our calculations is orbitally asymmetric, in which a large orbital polarization can exist in the metallic phase. Based on the obtained phase diagram shown in Fig. 4, we find that the orbital squared moments are finite when the system is metallic or in the OSMP, whereas a zero squared moment $\langle T_z^2 \rangle = 0$ corresponds to the insulating phase. As a result, the $U$ dependence of the squared moment $\langle T_z^2 \rangle$ displays a stair-step profile with a quickly drop point, which corresponds to the happening of the Mott transition.

It is worth noticing that there exists a platform in the $\langle T_z^2 \rangle$-$U$ curve within the interaction region 3.55 eV $\leqslant U <$ 3.75 eV, indicating that the orbital polarization is especially stable in the OSMP when $J_H = 0.25U$. Because the narrow $d_{3z^2-r^2}$ band with localized electron keeps half-filled in the OSMP, the itinerant electrons in the wide $d_{x^2-y^2}$ can not transfer to the lower Hubbard sub-band of the narrow orbital, leading the orbital polarization to be fixed. Therefore, the orbital

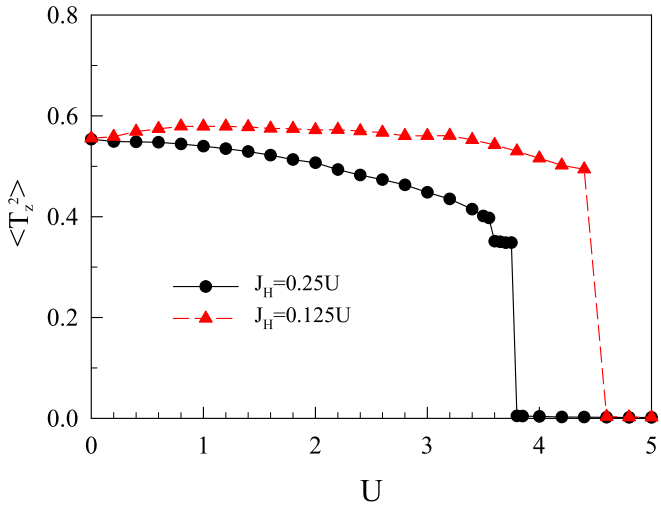


FIG. 9. $U$ dependence of the squared moment $\langle T_z^2 \rangle$ for different Hund's rule coupling $J_H = 0.25U$ (black line) and $J_H = 0.125U$ (red line) at half-filling.

polarization can also provide strong evidence for the occurrence of the OSMP.

The effect of the electron filling on the local orbital squared moments is presented in Fig. 10 for $Ba_2CuO_{4-\delta}$ when $2.0 \leqslant n_e \leqslant 2.5$. As shown in Fig. 10(a), the local orbital squared moments slightly increase with the increasing of electron filling when the system is in the metallic phase for $n_e > 2.2$. Near the half-filling region, the Hund's rule coupling plays an essential role: $\langle T_z^2 \rangle$ decreases with increasing $n_e$ for $J_H = 0.1U$, because more electrons transfer to the low-energy wide $d_{x^2-y^2}$ band when the system has a large crystal-field splitting and a small $J_H$ [36]. When the Hund's rule coupling increases to $J_H = 0.3U$, an OSMT happens when $n_e \leqslant 2.1$, and the squared moments keep almost unchanged in the OSMP. This can also be seen in Fig. 10(b).

Totally speaking, the orbital polarization is suppressed by the Hund's rule coupling in the metallic phase, but it becomes almost constant in the OSMP, as one sees in Figs. 10(a) and 10(b). As a result, the orbital polarizations in the OSMP

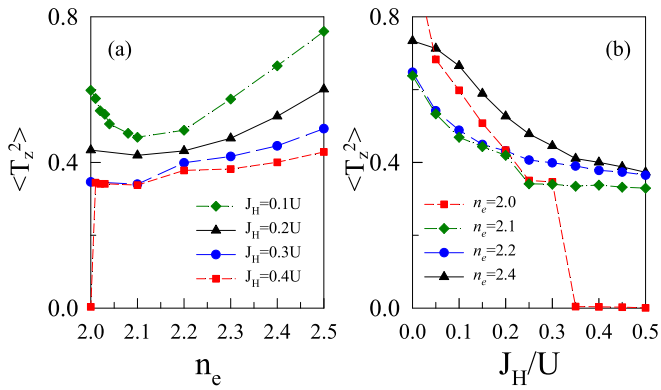


FIG. 10. Orbital polarization in the hole-overdoped $Ba_2CuO_{4-\delta}$ when $U = 3.6$ eV. (a) Local orbital squared moment as a function of $n_e$ for different Hund's rule couplings. (b) Comparing the $J_H$ dependencies of $\langle T_z^2 \rangle$ for different $n_e$.

or near the edge of the OSMP may be helpful for the occurrence of orbital-selective superconductivity in $Ba_2CuO_{4-\delta}$ compound [8]. Meanwhile, the orbital polarization in metallic phase does not lead to orbital order due to the absence of lattice distortion.

### D. Discussion

Thus far, we may expect that in the SC $Ba_2CuO_{4-\delta}$, there exist two types of electrons: the narrow-band electrons near the edge of the Mott localized state, and the wide-band electrons, resemble to an earlier two-band hypothesis by Xiang *et al.* [37]. Intuitively the multiorbital model for HTSC cuprates is more reasonable than the single-orbital model: in conventional BCS superconductors, the ionic background and phononic vibrations provide the SC pairing force field of Cooper pairs, and paired carriers are responsible for carrying the supercurrent; in contrast, the carriers of the single-orbital $t$-$J$ model play duplicate roles, they not only create spin fluctuations to provide a SC pairing force but also carry a supercurrent. Thus, the single-orbital $t$-$J$ model leads to a dilemma: the creation of the pairing force and carrying of the supercurrent are competitive; the more the carriers participate in spin fluctuations, the less the carriers participate in carrying the supercurrent, and vice versa [38–40]. As a comparison, a multiorbital superconductor could avoid such a difficulty: the electrons in one or two orbitals can contribute spin or orbital fluctuations, and electrons in another one or two orbitals contribute SC pairs and carry supercurrent. In the same time, the multiorbital and OSMP characters of the compressed compound $Ba_2CuO_{4-\delta}$, as well as of the compound $Sr_2CuO_{4-\delta}$, imply that the spin fluctuations along with the orbital fluctuations may enhance the SC pairing force and greatly lift $T_c$ in $Ba_2CuO_{4-\delta}$ and $Sr_2CuO_{4-\delta}$, resembling to multiorbital high-$T_c$ iron pnictide superconductors. Thus one could understand why the SC critical temperatures of $Ba_2CuO_{4-\delta}$ and $Sr_2CuO_{4-\delta}$ are about 70 and 90 K, significantly larger than those of $La_2CuO_{4-\delta}$, which is about 30–40 K.

## IV. CONCLUSIONS

In summary, we study the orbital selectivity of the effective two-orbital Hubbard model of $Ba_2CuO_{4-\delta}$ compound by using the dynamical mean-field theory with the Lanczos method as the impurity solver. We demonstrate that $Ba_2CuO_{4-\delta}$ is an OSMP compound at half-filling or is near the edge of the OSMP in the optimal hole-doping region, and a stable orbital polarization can be observed in the OSMP regime. These suggest that a local magnetic moment and spin or orbital fluctuations still exist, and the OSMP and the orbital polarization are significant features of the hole-overdoped $Ba_2CuO_{4-\delta}$. Our results are also applicable to $Sr_2CuO_{4-\delta}$ and other two-orbital cuprates. Regarding the half-filled $Ba_2CuO_{3.5}$ as the parent phase, our work provides a new perspective to understand the physics in the superconducting $Ba_2CuO_{4-\delta}$.

## ACKNOWLEDGMENTS

This work is supported by the National Natural Science Foundation of China (NSFC) under the Grants No. 11474023, No. 11774350, and No. 11174036.

[1] W. M. Li, J. F. Zhao, L. P. Cao, Z. Hu, Q. Z. Huang, X. C. Wang, Y. Liu, G. Q. Zhao, J. Zhang, Q. Q. Liu, R. Z. Yu, Y. W. Long, H. Wu, H. J. Lin, C. T. Chen, Z. Li, Z. Z. Gong, Z. Guguchia, J. S. Kim, G. R. Stewart *et al.* Proc. Natl. Acad. Sci. USA **116**, 12156 (2019).

[2] Q. Q. Liu, H. Yang, X. M. Qin, Y. Yu, L. X. Yang, F. Y. Li, R. C. Yu, C. Q. Jin, and S. Uchida, Phys. Rev. B **74**, 100506(R) (2006).

[3] W. B. Gao, Q. Q. Liu, L. X. Yang, Y. Yu, F. Y. Li, C. Q. Jin, and S. Uchida, Phys. Rev. B **80**, 094523 (2009).

[4] P. D. Han, L. Chang, and D. A. Payne, Physica C **228**, 129 (1994).

[5] F. C. Zhang and T. M. Rice, Phys. Rev. B **37**, 3759 (1988).

[6] K. J. von Szczepanski, T. M. Rice, and F. C. Zhang, Europhys. Lett. **8**, 797 (1989).

[7] N. P. Armitage, P. Fournier, and R. L. Greene, Rev. Mod. Phys. **82**, 2421 (2010).

[8] T. Maier, T. Berlijn, and D. J. Scalapino, Phys. Rev. B **99**, 224515 (2019).

[9] K. Jiang, X. Wu, J. Hu, and Z. Wang, Phys. Rev. Lett. **121**, 227002 (2018).

[10] K. Liu, Z.-Y. Lu, and T. Xiang, Phys. Rev. Mater. **3**, 044802 (2019).

[11] Z. Wang, S. Zhou, W. Chen, and F.-C. Zhang, Phys. Rev. B **101**, 180509(R) (2020).

[12] Y. Li, S. Du, Z.-Y. Weng, and Z. Liu, Phys. Rev. Mater. **4**, 044801 (2020).

[13] A. Georges, G. Kotliar, W. Krauth, and M. J. Rozenberg, Rev. Mod. Phys. **68**, 13 (1996).

[14] G. Kotliar, S. Y. Savrasov, K. Haule, V. S. Oudovenko, O. Parcollet, and C. A. Marianetti, Rev. Mod. Phys. **78**, 865 (2006).

[15] G. Rohringer, H. Hafermann, A. Toschi, A. A. Katanin, A. E. Antipov, M. I. Katsnelson, A. I. Lichtenstein, A. N. Rubtsov, and K. Held, Rev. Mod. Phys. **90**, 025003 (2018).

[16] A. M. Oleś, Phys. Rev. B **28**, 327 (1983).

[17] A. Koga, N. Kawakami, T. M. Rice, and M. Sigrist, Phys. Rev. B **72**, 045128 (2005).

[18] E. Dagotto, Rev. Mod. Phys. **66**, 763 (1994).

[19] M. Caffarel and W. Krauth, Phys. Rev. Lett. **72**, 1545 (1994).

[20] M. Capone, L. de' Medici, and A. Georges, Phys. Rev. B **76**, 245116 (2007).

[21] Y. Niu, J. Sun, Y. Ni, J. Liu, Y. Song, and S. Feng, Phys. Rev. B **100**, 075158 (2019).

[22] F. Lu, W.-H. Wang, and L.-J. Zou, Phys. Rev. B **77**, 125117 (2008).

[23] C. A. Perroni, H. Ishida, and A. Liebsch, Phys. Rev. B **75**, 045125 (2007).

[24] E. Jakobi, N. Blümer, and P. van Dongen, Phys. Rev. B **80**, 115109 (2009).

[25] A. Koga, N. Kawakami, T. M. Rice, and M. Sigrist, Phys. Rev. Lett. **92**, 216402 (2004).

[26] V. I. Anisimov, I. A. Nekrasov, D. E. Kondakov, T. M. Rice, and M. Sigrist, Eur. Phys. J. B **25**, 191 (2002).

[27] Y. K. Niu, J. Sun, Y. Ni, and Y. Song, Physica B **539**, 106 (2018).

[28] J. Sun, Y. Liu, and Y. Song, Acta Phys. Sin. **64**, 247101 (2015).

[29] T. A. Costi and A. Liebsch, Phys. Rev. Lett. **99**, 236404 (2007).

[30] L. de' Medici, J. Mravlje, and A. Georges, Phys. Rev. Lett. **107**, 256401 (2011).

[31] A. Georges, L. de' Medici, and J. Mravlje, Annu. Rev. Condens. Matter Phys. **4**, 137 (2013).

[32] A. Liebsch, Phys. Rev. Lett. **95**, 116402 (2005).

[33] L. de' Medici, Phys. Rev. B **83**, 205112 (2011).

[34] E. Jakobi, N. Blümer, and P. van Dongen, Phys. Rev. B **87**, 205135 (2013).

[35] L. de' Medici, S. R. Hassan, M. Capone, and X. Dai, Phys. Rev. Lett. **102**, 126401 (2009).

[36] J. Zaanen and A. M. Oleś, Phys. Rev. B **48**, 7197 (1993).

[37] T. Xiang, H. G. Luo, D. H. Lu, K. M. Shen, and Z. X. Shen, Phys. Rev. B **79**, 014524 (2009).

[38] T. Jarlborg, B. Barbiellini, R. S. Markiewicz, and A. Bansil, Phys. Rev. B **86**, 235111 (2012).

[39] C. de Graaf and F. Illas, Phys. Rev. B **63**, 014404 (2000).

[40] J. Zaanen, G. A. Sawatzky, and J. W. Allen, Phys. Rev. Lett. **55**, 418 (1985).